

RSC Advances



This is an *Accepted Manuscript*, which has been through the Royal Society of Chemistry peer review process and has been accepted for publication.

Accepted Manuscripts are published online shortly after acceptance, before technical editing, formatting and proof reading. Using this free service, authors can make their results available to the community, in citable form, before we publish the edited article. This *Accepted Manuscript* will be replaced by the edited, formatted and paginated article as soon as this is available.

You can find more information about *Accepted Manuscripts* in the [Information for Authors](#).

Please note that technical editing may introduce minor changes to the text and/or graphics, which may alter content. The journal's standard [Terms & Conditions](#) and the [Ethical guidelines](#) still apply. In no event shall the Royal Society of Chemistry be held responsible for any errors or omissions in this *Accepted Manuscript* or any consequences arising from the use of any information it contains.

ARTICLE

Photo and Electronic Excitation for Low Temperature Catalysis over Metal Nanoparticles via Organic Semiconductor

Cite this: DOI: 10.1039/x0xx00000x

Weiran Zheng^{a,b}, Simon Jones^a, Xinlin Hong^b, Shik Chi Edman Tsang^{a*}

Received 00th January 2012,
Accepted 00th January 2012

DOI: 10.1039/x0xx00000x

www.rsc.org/

Simple supported metal catalysts are active for the destruction of a wide range of hazardous chemicals of environmental concerns including CO, N₂O and volatile organic compounds (VOCs) in air at elevated temperature but severely restricted due to unfavourable enthalpy, intrinsic low activity at ambient conditions, particularly the inapplicability of using high temperature in confined space. Here, we report that a simple but significant mean of electron promotion to metal nanoparticle by the use of organic polythiophene polymer as support or support supplement, which gives rise to active modified metal surface for selective catalysis at low temperature with light or electromotive excitations. It is shown that the finite size of electronic structure of dispersed metal nanoparticles can be influenced by the conjugative bands of the polymer, which lead to modification of its adsorptive properties. This renders the composite material active for a number of oxidation and decomposition reactions to be taken place at ambient conditions, which outclasses the performance of conventional catalysts. As a result, the present study forms a basis for further developments in the design and engineering of a new class of *Greener plastic nanocatalysts* with facilitated electron promotion to metal catalysts for environmental relevant chemical transformations.

Introduction

The pollution problems associated with industrialization in many developing countries have become stringent over the past few years. The release of industrial toxic and hazardous chemical substances to air, soil and water in some regions has caused a catastrophic change to environment.¹ For example, the recent severe smog problems in Chinese cities due to a poor control in emissions have triggered alarms to local governments regarding health and safety in their living environment. Additionally, the sudden built-up of a local high concentration of unwelcome gases such as CO and VOCs in confined buildings (generally known as 'building sickness'), living rooms, toilets and vehicles due to cigarettes, poor means of heating and contaminations in furniture may also induce health concerns. In order to address these problems, extensive research is currently underway to develop advanced analytical, biochemical, and physicochemical methods for the characterization and elimination of hazardous chemical

compounds from air, soil, and water. Development of advanced materials for low (ambient) temperature but selective catalysis is regarded to be more superior to conventional approaches such as absorption or high temperature incineration process due to more favourable enthalpy, ease of processing and regeneration and in some cases, the inapplicability of using high temperature in confined space. The versatile employment of metal nanoparticles as catalysts for destruction of hazardous chemicals is a well-accepted method as small metal phase shows high activity in catalytic oxidation at elevated temperature.² For example, catalytic combustion of CO and destruction of volatile organic compounds (VOCs) in air over supported metal nanoparticles have been extensively studied. However, conventional supported metal catalysts are generally not active at ambient conditions unless heat or additional means of activation such as use of magnetic, electromotive or optical force to promote catalysis is applied.³ The use of solar energy for pollution control has also been recently explored. Placing

metal nanoparticles on inorganic transition metal semiconductor oxides such as TiO₂ and ZnO is perhaps the most common way to harness the solar energy to enable electronic promotion to the metal particles. But characteristic bandgap of typical transition metal oxide matches the ultraviolet radiation with generally lower absorptivity of the materials to the solar region. In addition, electronic promotion of metal nanoparticles using electromotive force would require highly conductive material to reduce ohmic loss of energy hence most commonly used transition metal oxides are not ideal in these respects.

We have recently observed a significant degree of electronic perturbation to small Pd nanoparticle by the partial adsorption of pendant NH₂ or OH groups (contributing their lone pair electrons to enhance electron density of metal for molecular adsorption) of rigid polymer support in a close proximity under ambient conditions due to high surface coverage and also with a finite number of metallic electrons involved.⁴ This may suggest catalysis by metal nanoparticles could be significantly promoted by organic moiety groups for low temperature applications but there is very limited work in this area. On the other hand, recent research on the use of organic polymer semiconductors such as polypyrrole, polyparaphenylene and polythiophene (PTh) to give useful electronic, optical and magnetic properties is rapidly increasing.^{5,6} Conjugated systems formed by p_z orbitals of polymer semiconductors plays a key role in altering the band structures of the materials, while the π-π* transitions lie typically between 1.5 and 3 eV resulting in visible light absorption or emission.⁵ Comparing to inorganic semiconductors, the band structures of polymer semiconductors are significantly narrower but with effective overlapping of orbitals in symmetry, which generally lead to a higher efficiency of capturing solar energy.⁷ In addition, the bandgap and conductivity are also temperature sensitive and can be engineered by morphology and function groups of the polymers.⁸ As a result, the use of polymer semiconductors has been widely studied as a key component in photocatalysts, such as photoevolution of H₂^{9,10}, photocatalytic fixation of CO₂¹¹ and numerous degradation reactions¹². As similar to inorganic semiconductors such as TiO₂ incorporation of metal nanoparticles such as Au, Ag, Pd is commonly used to modify the properties of these conjugated polymers hence further extending their potential usages as electronic devices, sensor, catalyst and solar cells, etc., the hydrogenation of unsaturated organic molecules were one of the most referred examples.¹³⁻¹⁹ By forming hybrid materials of inorganic/polymer semiconductors, charge transfer from/to polymer were observed along with enhancement of carrier lifetime and interface properties.²⁰ Theoretical study of metal/organic semiconductor interface was also extensively studied.²¹ These hybrid materials have been briefly studied as electrocatalysts^{22,23,24} and catalysts for organic hydrogenation reactions^{18,25}. Despite the above studies on the modification of conductive polymer by the metal particles, the reverse scenario: the use of polymer semiconductors as support to modify metal nanoparticles, its usage in energy and hazard gas destruction, particularly as

photocatalytic decomposition at low temperature is still not yet systematically explored, especially in gas phase reactions²⁶.

In this paper, we report a simple but significant mean for electronic promotion to Pd nanoparticles by using polythiophene polymer as a support. Notice that the term 'electronic promotion refers to the electronic interaction between metal and conducting polymer, which promotes photo and electro-catalysis at low temperature (not the electron flow direction in any specific electrochemical reactions).

It is hereby demonstrated that the new composite material can catalyse combustion and decomposition of toxic gases and VOCs of environmental concerns significantly at room temperature in the presence of light or electromotive force. As a result, catalytic decomposition of formic acid (HCOOH), destruction of toxic nitrous oxide (N₂O) in hydrogen as well as selective carbon monoxide (CO) oxidation in air can be effectively promoted at ambient conditions. It is also clearly evident from CO-stripping voltammetry, X-ray photoelectron spectroscopy and infrared spectroscopy that a strong charge transfer between metal nanoparticles and polymer semiconductor can take place at their interface through the thio-metal surface interaction. This preliminary work clearly supports the fact that organic semiconductor polymeric materials could be employed as substituent or additive to conventional inorganic support to host metal nanoparticles for low temperature catalytic destruction of toxic gases with the energy input from light or electrical means. Thus, this may open up a possibility of developing a new technology of using flexible metal supported plastic nanocatalysts for pollution treatment.

Experimental

Chemicals

Thiophene, Palladium(II) nitrate, Silver nitrate, chloroform, ethanol, Polyvinylpyrrolidone (PVP, M_w=33,000), Iron(III) chloride, and 65 wt% hydrazine (N₂H₄) in water were purchased from Sigma-Aldrich and used as received. Amorphous carbon powder (Type 87L) was supplied by Johnson Matthey.

Synthesis of polythiophene (PTh)

Thiophene (2.68 g) was dissolved in a solution of chloroform (100 mL) in a 500mL reaction vessel and kept at 0 °C in ice bath. FeCl₃ (20.67 g) was dissolved in 100 mL of chloroform and was added dropwise into previous solution. The mixture was kept at 0 °C for 16 h and consistently stirred at 600 rpm. The solution colour changed from orange to dark green after 10 min. Then the mixture was centrifuged and washed with ethanol and Distilled (DI) water for 5 times, the colour changed to dark red once mixed with ethanol because of reduction of oxidized PTh. The solid was further collected and dried in air at 60 °C for 24 h. 1.46 g PTh was obtained afterward, with a yield of 54.5%.

Synthesis of Pd/PTh-C, Ag/PTh and Ag-Pd/PTh-C

For the synthesis of 10 wt% Pd/PTh-C, certain ratio of amorphous carbon powder and polythiophene were mixed in 50 mL ethanol, followed by ultrasonic dispersion at 30 °C for 1 h, and then cooled down to 5 °C. 50 mg of Pd(NO₃)₂•2H₂O was dissolved in the solution, then the solution was refluxed at 80 °C for 1h for the complete reduction of Pd²⁺ to Pd⁰ by ethanol. The suspension was filtered and the solid was further washed by DI water, then collected and dry under 60 °C for 24 h before use. The preparation of Ag/PTh was done by mixing 28.7 mg of AgNO₃ with polythiophene in water, followed by adding 50.48 μL of 65 wt% N₂H₄•H₂O solution dropwisely. The mixture was stirred in room temperature (RT) for 30 min. The suspension was filtered and washed with ethanol and DI water, then dried under 60 °C for 24 h. Ag-Pd/PTh-C was prepared as follows: 300 mg Pd/C or Pd/PTh-C catalyst was weighted and mixed with 200 mL of DI water. The solution was bubbled H₂ for 30 min. 28.7 mg of AgNO₃ was dissolved in water and the solution was added into above mixture and kept stirring for 30 min under RT. Then, 50.48 μL of 65wt% N₂H₄•H₂O solution was added dropwise and stirred at RT for 30 min. The mixture was filtered and further washed by DI water, then collected and dry under 60 °C for 24 h before use.

Characterization

Powder X-Ray Diffraction (XRD): XRD analysis was performed using a PANalytical X'Pert Pro diffractometer, operating in Bragg-Brentano focusing geometry and using Cu_{Kα} radiation ($\lambda = 1.5418 \text{ \AA}$) from a generator operating at 40 kV and 40 mA.

CO pulse chemisorption: The test was carried out on a ChemBET Pulsar TPR/TPD Automated Chemisorption Analyser by Quantachrome instruments. 30 mg of catalyst was used and well filled into a quartz tube. Carrier gas was N₂ (20 mL/min). H₂ was flowed over the catalyst for 1 h at 40 °C to reduce remaining PdO and remove physically adsorbed molecules before CO pulse. Once the sample was cooled down to RT and TCD detector remained stable for 10 min under N₂, CO pulse was started. Analysis was stopped when no significant difference was observed in neighbour 3 peaks.

CO stripping voltammetry: Compactstat electrochemical interface provided by IVIUM technologies was used. Before experiment, glassy carbon (GC) electrode surface was polished with 0.3 mm alumina slurry, and then rinsed with doubly distilled water in ultrasonic bath. Then 400μL DI water was mixed with 10 mg of catalyst, followed by adding 30 μL of 5 wt% Perfluorosulfonic acid-Polytetrafluoroethylene (PTFE) copolymer solution. The mixture was ultrasonic dispersed for 1 h. Then 10 μL of prepared ink was dropped on to the GC surface and dry under vacuum for 1 h. the GC electrode was exposed to saturated CO at 0.2 V and followed by washing with 0.5 M H₂SO₄ with pre-treatment of N₂. The test was carried out in 0.5 M H₂SO₄ saturated with N₂. First two cycles were recorded at a scan rate of 10mV/s with saturated calomel

electrode (SCE) as reference electrode, and the whole system was kept at RT and dark.

Thermogravimetric analysis: The analysis was done on Q50 TA thermogravimetric analysis system. Certain amount of catalyst was used, then the analysis was carried out in air. The heating rate was 5 °C/min.

Attenuated Total Reflectance Fourier Transform Infrared Spectroscopy: ATR-IR was done on NICOLET 6700 instrument from Thermo Scientific. PVP stabilized Pd was synthesized in ethylene glycol under 180 °C using Pd(NO₃)₂•2H₂O as metal precursor. The colloidal Pd nanoparticle was divided into two parts and dispersed in ethanol. One was mixed with 3 wt% of polythiophene and further ultrasonic disperse for 2 h under 50 °C. Then H₂ was passed through both solution for 1 h to fully reduce the nanoparticles. After that, CO was bubbled for 1h. Then, the resulting ink solution was dropped on ATR crystal and left dry in N₂ for 1 h before the sample spectra were collected. When light was used, the sample spectra were collected 1 h after light was on.

Hydrogen Evolution Reaction (HER) activity test: The curves were measured on Compactstat electrochemical interface provided by IVIUM technologies. 400 μL DI water was mixed with 10 mg of catalyst and 30 μL of 5 wt% Perfluorosulfonic acid-PTFE copolymer solution. The mixture was ultrasonic dispersed for 1 h. Then 10 μL of prepared ink was dropped on to the GC surface and dried under vacuum for 1 h. The GC electrode was further cleaned by 20 cycles of voltammetry scanning between -0.2 V and 1.0 V. Then the hydrogen evolution reaction was performed from 0.1 V to -0.6 V at a rate of 10 mV/s with saturated calomel electrode (SCE) as the reference electrode. All tests were carried out under RT.

Ultraviolet-visible reflectance spectroscopy: The reflectance spectra were achieved on PerkinElmer Lambda 750S. Resolution was set at 1 nm. KBr was mixed with the sample with a weight ratio of 500:1.

Raman spectroscopy: Raman characterization was done on PerkinElmer RamanStation 400F. The intensity of laser was set at 5% to avoid destroy of polymer structure. Total scan time was 60 s.

Gas chromatography: Gas chromatography was used to analyse the gas produced by catalytic reactions. Two TCD detectors was involved one using N₂ as carrier gas to detect H₂, another one using helium (He) as carrier gas to detect CO, O₂, CO₂ and N₂O.

Catalytic test condition

Formic acid decomposition: The tests were evaluated in a quartz reactor and kept at target temperature. Gas outlet was connected to gas measurer and recorded once 10 mL of 50 vol% formic acid solution was mixed with 50 mg of catalyst.

CO oxidation: CO oxidation reactions were evaluated in a quartz reactor of 50 mL at 0.3 bar using 50 mg of catalyst with a mixture gas of 2.60% CO and 5.0% O₂ in He. The reactor was sealed and pressure was maintained at 0.3 bar. With and

without irradiation, the concentration of CO₂, CO and O₂ was analysed by gas chromatograph using He as carrier gas.

N₂O decomposition: N₂O decomposition reactions were performed in a quartz reactor of 50 mL with 50 mg of Pd/C and Pd/2 wt%PTh/C with and without irradiation. The reactor was kept at 0.3 bar, with 2500 ppm N₂O and 4.75% Ar in 95% H₂. Whole set was kept at RT.

Transmission electron microscopy (TEM) and Scanning electron microscope (SEM): TEM was done on JEOL 2000FX, a drop of diluted water solution with catalyst was dried on carbon copper grid to prepare the sample. SEM was done on Hitachi S-4300 scanning electron microscope, with Au coating samples.

X-ray Photoelectron Spectroscopy (XPS): XPS was performed in a VG Microtec ion pumped XPS system equipped with a nine channel CLAM4 electron energy analyzer. 200 watt Mg X-ray excitation was used. The samples were analysed with reference to adventitious C_{1s} peak.

Results and discussion

Structure and properties

Polythiophene (PTh) was synthesized using FeCl₃ as catalyst to induce polymerization of thiophene monomers according to literature process²⁷ with modification, then palladium nitrate dehydrate was dissolved in a mixed suspension of PTh and amorphous carbon followed by reduction with ethanol at low temperature. As a result, 10 wt% of Pd nanoparticle was loaded on the support which contained PTh ranged from 0.5 to 100 wt%. Although Pd-PTh on amorphous carbon was mainly studied as catalyst, the high proportion of the amorphous carbon can obscure the structural aspects of Pd-PTh. Thus, XRD and TEM of Pd-PTh without support were characterized. The XRD and TEM (Fig. S1 to S3) showed the crystalline size of Pd nanoparticles on all mixed supports was 4.5±0.9 nm, while the mean size of Pd nanoparticles supporting on 100% PTh was 6.03 nm. The particle size increased gradually with the addition of PTh (Table 1). The morphology of polymer appeared to be in laminated sheet-like structure (Fig. 1a, 1b), and there was no significant change in morphology upon the addition of Pd (Fig. 1e). The apparent metal area of Pd derived from CO chemisorption decreased progressively with increasing PTh content. It was because the increasing amount of sulfur atoms from thiophene blocked the access of Pd surface, leading to poisoning of the exposed metal sites. Unlike flexible polymer like polyvinylpyrrolidone (PVP) studied, polythiophene was a rigid polymer (sheet like) due to the π -conjugate systems across the polymer backbone. Thus, even when the weight ratio of PTh was risen to 20 wt% with the molar ratio of Pd to sulphur at 1: 2.53, the metal surface area was only dropped from 5.36 to 1.09 m²/g. On the other hand, no chemisorption of CO was observed indicating that the Pd surface was entirely covered by the polythiophene when 100% PTh was used. Noticeably, the Pd surface area slightly increased from 5.36 to 6.99 m²/g when 0.5 wt% PTh was added

into carbon support. This could be caused by the change of the morphology of Pd nanoparticles on the carbon internal surface such that the polymer with higher affinity for metal surface may have freed some surface of Pd particles from deep burying inside the amorphous carbon. The crystalline structures of PTh nanoparticles and Pd/PTh materials were also studied (Fig. 2a), two broad peaks were clearly observed at $2\theta \approx 21.1^\circ$ and 25.3° , both corresponding to chain-to-chain stacking²⁸. The d-spacing calculated based on the observed peaks was approximately 0.351-0.402 nm, which was in good agreement with TEM images, as shown in Fig. 2b. A few weak peaks were also shown in XRD pattern, indicating the existence of intermolecular ordered stacking structures. After the addition of Pd nanoparticles, the peaks of Pd nanoparticles were also observed. But the peak intensity at $2\theta \approx 25.3^\circ$ was attenuated suggesting that a degree of the chain-to-chain stacking of polymer sheets was disrupted due to the deposited Pd nanoparticles. The peak was also slightly shifted to lower angle indicative of a longer equilibrium distance of stacked chains due to the presence of Pd nanoparticles.

PTh percentage / %	Pd/PTh Molar ratio	Pd surface area / m ² g ⁻¹ catalyst	Mean Pd particle size / nm
0	1:0	5.36	4.16
0.5	1:0.06	6.99	4.21
1	1:0.13	4.46	4.07
2	1:0.25	4.37	4.32
5	1:0.63	3.58	5.18
10	1:1.27	2.59	5.58
20	1:2.53	1.09	6.21
100	1:12.7	0.01	6.03

Table 1 Pd surface areas of 10wt% Pd on PTh-C support with different contents. Pd surface area was measured by CO pulse chemisorption and mean Pd particle size was characterized by TEM images.

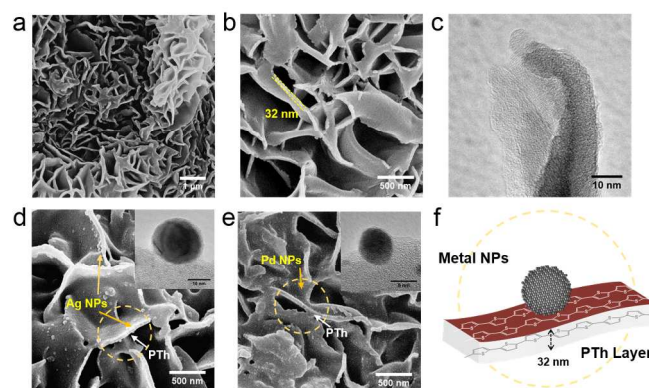


Fig. 1 (a) & (b) SEM images, (c) TEM image of layered structure of polythiophene; (d) SEM image of Ag/polythiophene; (e) SEM image of Pd/polythiophene; the inserts of (d) and (e) are corresponding TEM images of metal particles; (f) a pictorial illustration of metal-polythiophene hybrid structure.

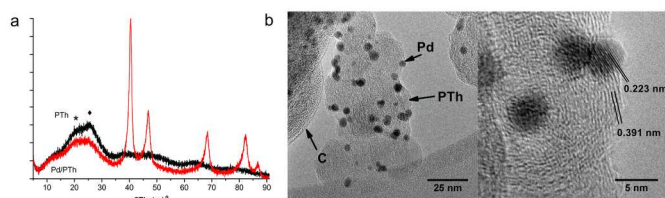


Fig. 2 (a) XRD pattern of PTh powder and 10 wt% Pd/PTh catalyst. (b) TEM images of 10 wt% Pd/5 wt% PTh-C catalyst.

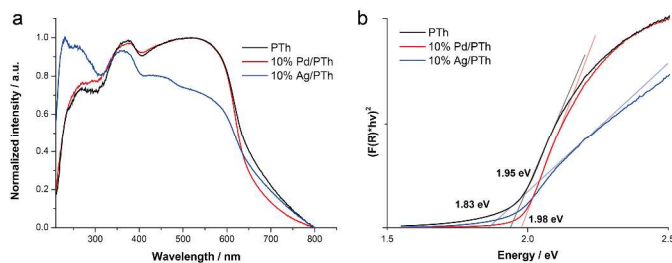


Fig. 3 (a) UV/Vis diffuse reflectance spectra of PTh particles and 10 wt% Pd/PTh; (b) Kubelka-Munk equation plots of corresponding UV/Vis spectra, see SI for equation.

It is well accepted that polythiophene is an organic semiconductor with a narrow bandgap.⁵ As seen from the Fig. 3 that the calculated bandgap from its UV/Vis diffuse reflectance spectrum of our synthetic polythiophene is shown to be 1.95 ± 0.01 eV (this band structure has been extensively studied and presented in literature as 1.96 eV²⁹) using Kubelka-Munk equation. This corresponds to the energy of a visible photon with wavelength of 636 nm. Three local absorption peaks are clearly shown in the UV/Vis spectra of PTh: the first peak at 276 nm is attributed to $n-\pi^*$ of thiophene rings; the second peak at 379 nm to $\pi-\pi^*$ of thiophene rings and the third strongest broad peak from 455 nm to 635 nm to $\pi-\pi^*$ of conjugated polymer backbone. The position of the broadened adsorption edge is known to reflect the extent of electron conjugation and the coexistence of different chain lengths of conjugation system within the PTh sheets²⁷. After in-situ reduction, Pd nanoparticles were formed on the surface of PTh polymer, the three peaks were remained unchanged but there was a clear extension of the absorption edge towards a shorter wavelength compared to the sample without Pd from the UV/Vis spectra. This suggests that the conjugated structure of PTh was perturbed by the Pd. The calculation indicated that the bandgap of PTh was significantly shifted when Pd nanoparticles were introduced: from 1.95 ± 0.01 eV to 1.98 ± 0.01 eV. Thus, the typical Schottky junction with electronic interaction between polymer chains and Pd nanoparticles is apparent, which appears to enlarge the bandgap value of polymer by removing excited electrons from the polymer to the Pd metal. However, when Ag nanoparticles were doped to the polymer, the bandgap this time was substantially reduced to 1.83 ± 0.01 eV indicating that excited electron injection from Ag nanoparticles (plasmonic effect) to the polymer (also induced peak shifts in the UV-Vis spectrum). In addition, two

new peaks in the UV/Vis spectrum were shown at 220 nm and 450 nm, corresponding to the adsorption edge of Ag nanoparticles and surface plasmon resonance (SPR) peak of Ag nanoparticles, respectively. Thus, there is a clear electron interaction between the metal and the PTh. Further probing of electronic interaction between Pd and neighbour atoms of the PTh by synchrotron XPS could be useful. Notice that there was no apparent change in the peak number and peak shape of fundamental Raman vibration spectra with and without the incorporation of metal (either Pd or Ag) indicative of the good stability of the polymer (see Fig. S4 and Table. S1).

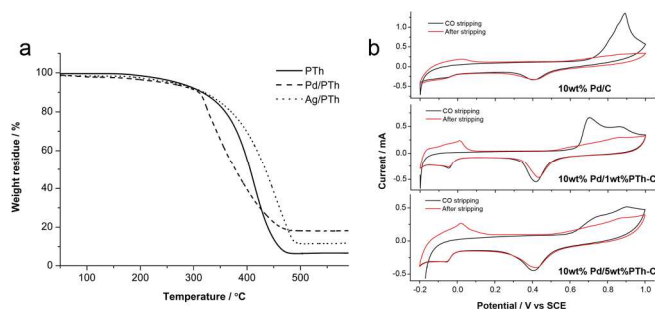


Fig 4 (a) TGA curves of PTh and 10 wt% metal loaded PTh samples: 10 wt% Ag/PTh and 10 wt% Pd/PTh, in air atmosphere; (b) CO_{ads} stripping voltammograms at 10 wt% Pd with different supports in 0.5 M H_2SO_4 solution after exposed to saturated CO at 0.2 V: Pd/C catalyst; Pd/1 wt% PTh-C catalyst and Pd/5 wt% PTh-C catalyst. First cycle shown in dark line, and second cycle in red line to illustrate the total oxidation of adsorbed CO during stripping.

Considering the employment of polymer as catalyst support its thermal stability is of a main concern. Thermogravimetric analysis (TGA) shown in Fig. 4a depicts that PTh remains stable until 300°C, followed by its gradually decomposition in air with the completion of the process at 480°C. The doping of Pd nanoparticles clearly reduces the decomposition temperature by about 40°C suggesting a catalytic effect. In contrast, for the Ag doped PTh, the decomposition temperature apparently increases. It is clear that Pd nanoparticles can accept excited electrons from polymer from the positive charge transfer hence attenuating the stability of polythiophene. This facilitates to a stronger surface adsorption of the polymer, which leads to catalytic cleavage of the organic structure on the Pd metal surface.⁴ On the other hand, we observe that Ag with a higher band energy than Pd, can donate electrons to the polythiophene, (negative charge transfer) rendering the conjugated structure more stable. Thus, it is concluded that metal nanoparticles can exert a strong electronic interaction with the polymer as shown above. In this paper, further studies on Pd were carried out since most catalytic oxidation and decomposition reactions at low temperature would require electronic contribution from the catalytic metal surface to the adsorbate(s) for their consequential activation.

Electrochemical characterization of the Pd doped sample was therefore studied. CO-stripping voltammetry in 0.5 M H_2SO_4 was performed to evaluate CO tolerance and electro-oxidation of the Pd nanoparticles supported on the conductive polymer. Pure PTh showed no activity in the CO stripping and it can be seen from Fig.

4b that when CO stripping is performed over typical Pd/C material, hydrogen adsorption/desorption are taken place at the region from -0.1 V to 0 V. From the upper oxidation curve, preadsorbed CO on Pd is oxidized electrochemically by water at around 0.6 V to 1.0 V (max. at 0.9 V) with corresponding reduction of Pd-O at about 0.4 V in the lower reduction curve. Fig. 4b also clearly shows that in the presence of 1 wt% conducting polymer PTh, a new CO oxidation peak at lower onset potential of about 0.7 V arises. This new peak is attributed to the oxidation of CO on Pd but electronically modified directly from the underneath PTh polymer in parallel with the typical 0.9 V peak of Pd on carbon. The lower potential for the CO stripping indicates that Pd on PTh/C is electron richer than Pd/C. This information is consistent with the results obtained from the UV-vis reflectance and TGA. Noticeable, the relative size of lower potential peak of CO on Pd/PTh/C increases at the expense of high potential peak of CO on Pd/C when PTh reaches 5 wt%. Thus this suggests, with the addition of PTh the CO adsorption peak on Pd can be stripped off easier using lower potential, hence the composite material clearly shows a higher CO tolerance than unmodified one. On the other hand, Fig. S5 also show that the electrochemically active surface gradually decreases at increasing PTh content (total peak size), which is in agreement with the CO chemisorption result. Apparently, the thiophene moieties of PTh can block the Pd sites strongly from CO adsorption.

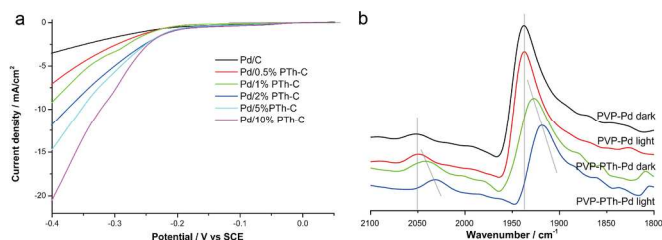


Fig. 5 (a) Hydrogen evolution reaction (HER) activities of 10 wt% Pd supported on PTh-C mixture in 0.1 M HClO_4 solution under 10 mV/s; (b) ATR-IR spectra of CO adsorption on polymer-stabilized colloidal Pd nanoparticles with and without exposure to light, PVP and PTh were used as stabilizers.

A comparison of polarization curves for the catalytic hydrogen evolution reaction (HER) from water for Pd/C with Pd/PTh/C at various compositions is shown in Fig. 5a. It was found that no hydrogen was produced on PTh/C or PTh. The addition of polythiophene dramatically increases the activity of Pd for the hydrogen production, giving higher hydrogen evolution rates. At a fixed potential of -0.4 V, the current density measured is 20.47 mA/cm² for Pd/ 10 wt% PTh/C compared to 3.48 mA/cm² for Pd/C. Bearing in mind that some active sites on Pd/PTh-C were blocked by the addition of PTh, the superior catalytic activity for hydrogen production of PTh modified Pd is prominent. We attribute to the higher intrinsic activity of PTh modified metal site and enhanced electron transfer using the conductive polymer. This clearly suggests that electrochemical catalytic activity can be promoted by using the PTh as a modifier.

ATR-FTIR using CO as surface probe was used to characterize the samples. Fig. 5b shows that two CO adsorption modes are identified: linear adsorption at 2054 cm⁻¹ and bridge mode at 1938 cm⁻¹,

respectively. Comparing to Pd on electrochemically inert polyvinylpyrrolidone polymer, the addition of 3 wt% of PTh to PVP stabilized Pd nanoparticles can induce a strong electron promotion to Pd. There are distinctive red shifts for both peaks with the CO bridge peak moving towards lower wavenumber of 1927 cm⁻¹ upon the addition of PTh (a shift of 11 cm⁻¹). The degree of metal surface coverage of CO was reported to affect the peak position of the bridge form due to different extent of dipole-dipole coupling³¹. After adding PTh to PVP-Pd colloid, we have found that the metal surface sites were reduced to 76% according to integrated peaks of the bridge form before and after the addition. As a result, a ¹³CO/¹²CO co-adsorption experiment was performed to appreciate the coverage effect and the actual shift caused by the electronic change due to PTh (Fig. S6). At the equivalent surface coverage the ¹²CO bridge peak (76%) of PVP-Pd was actually shifted from 1938 cm⁻¹ to 1934 cm⁻¹ (the position of ¹³CO bridge peak (24%) lied in the expected regime as previously reported³⁰), which is much smaller than those observed in the PVP-PTh-Pd sample. This clearly suggests that the majority of the CO shift is caused by the electronic donation of PTh to Pd where the contribution from CO dipole-dipole interaction is of less significance. Further red shift of this peak to 1918 cm⁻¹ can be seen from the figure when intense light is applied. In contrast, there is no equivalent peak shift for the PVP-Pd nanoparticles. This result yet again demonstrates that PTh can enhance electron density of Pd causing the red-shift of adsorbed CO modes (promote electron back donation to the CO). This could account for the facilitated CO oxidation at lower potential when PTh is used as support in the CO stripping voltammetry. In addition to the electrochemical promotion, radiation (The UV light source details is given in the supporting information) is no doubt to be another mean to excite the electron transfer from the semiconductor polymer to the Pd nanoparticle for catalysis. Sample characterizations by X-ray photoelectron spectroscopy were carried out and are shown in Figure S8. The spectra of polythiophene were also collected and used as a standard for comparison (Fig. S7-1). With the introduction of Pd, two pairs of spin-orbital coupling peaks of Pd could be clearly seen. The binding energy peaks of Pd^{II}3d_{5/2} and Pd^{II}3d_{3/2} (338.13 eV and 343.33 eV) were attributed to the Pd(II) directly bonded to S atom of polythiophene. The lower binding energy peaks of Pd⁰3d_{5/2} and Pd⁰3d_{3/2} (336.12 eV and 341.32 eV) corresponded to Pd nanoparticles without the direct contact of polythiophene presumably the particles were buried deep in the porous carbon structure (refer to CO stripping experiments). Also, it was found that there were two C_{1s} signals shown according to XPS spectrum, one could be attributed to amorphous carbon (285.10 eV) and the other to the C atoms from polythiophene (286.85 eV). The value of S2p_{3/2} peak was in a good agreement with literature value of thiophene compound with reference to the C_{1s}. In the case of Ag/PTh, only one pair of spin-orbital coupling peaks of Ag were observed due to the fact that the synthesised Ag particles, $30\sim 50$ nm from TEM (Fig. S3) and SEM, were considerably larger than Pd, without much ultrafine Ag nanoparticles within the porous carbon.

Catalytic Performance

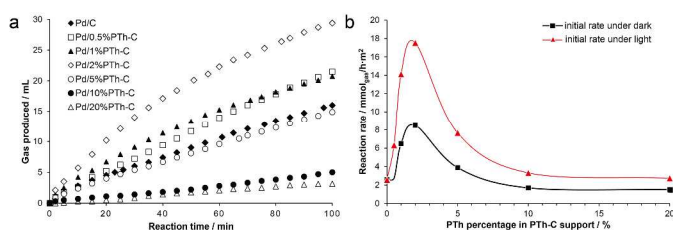


Fig. 6 (a) Formic acid decomposition over 10wt% Pd on different supports in dark: carbon support; 0.5wt% PTh in carbon; 1wt% PTh in carbon; 2wt% PTh in carbon; 5wt% PTh in carbon; 10wt% PTh in carbon; 20wt% PTh in carbon. (b) A plot of initial rate (measured at 3 min) vs PTh content in dark and light; 30 mg catalyst, 10 mL 50 vol% formic acid, 25 °C, 100 min.

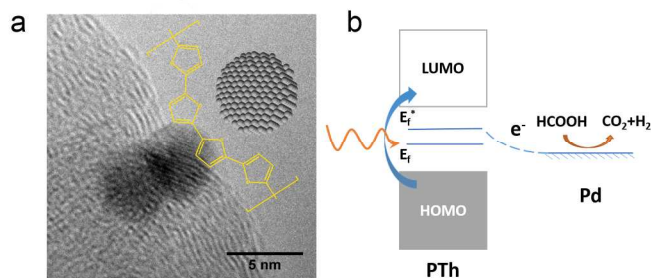


Fig. 7 (a) Illustration of Pd nanoparticle and PTH composite, (b) Electronic promotion effect of PTH on Pd in formic acid decomposition reaction when light is introduced to excite the semiconductor polymer.

Formic acid decomposition was employed to probe the catalytic activity of Pd nanoparticles on polythiophene. The catalytic activity of Pd was also measured with light illumination. Control experiments showed that pure PTH and PTH/C contributed no catalytic activity over formic acid decomposition, CO oxidation and N₂O decomposition with or without light illumination. It is known that higher electron density of promoted Pd can enhance the rate of formic acid decomposition due to stronger adsorption of the molecule by the electron back donation of the metal.⁴ Fig. 6a indeed shows that the initial rate of formic acid oxidation in dark condition increases from 2.59 mmol_{gas}h⁻¹m⁻²_{Pd} to 8.48 mmol_{gas}h⁻¹m⁻²_{Pd} when 2 wt% PTH is added to the Pd/C, suggesting a strong electronic promotion from polythiophene to Pd nanoparticles. Despite the fact that the rate is normalized per metal site exposed to discount the effect of metal site blocking by the support, further increase in PTH content can substantially reduce the rate indicative of electron withdrawing from excessive S atoms adsorption (Fig. 6b). Upon light illumination as an energy input, it is clearly observed that the catalytic rates of PTH containing samples are dramatically enhanced but not for the Pd/C sample without PTH. The optimal rate is found to be 17.5 mmol_{gas}h⁻¹m⁻²_{Pd} with the 2 wt% PTH sample when light is applied, which is more than double than the rate of the same catalyst in the dark. According to the model proposed by Kazuhiko Seki³⁰ (Fig. 7), the Fermi level of PTH is higher than that of Pd. Thus polythiophene with bandgap of 1.99 eV is clearly capable of adsorbing photon energy and promoting its π-electrons of the PTH to metal via the sulphur adsorption. More detailed reaction data and metal surface areas measured are compiled in supporting information

(Table S2). It has been reported³² that the electron rich Ag could render Pd more active for formic acid decomposition. Thus, AgPd with and without modification of polythiophene were tested. Table S2 clearly shows that the bimetallic catalyst is indeed more active than Pd. The increase in temperature also results in a higher apparent reaction rate. Thus, the combination of using Ag-Pd bimetallic nanoparticles, blending 2 wt% PTH to carbon support, light illumination and at a slight elevated temperature (40°C), more superior initial activity of 122.3 mmol_{gas}h⁻¹m⁻²_{Pd} (TOF=2927 h⁻¹) than most reported values in the literature. This clearly suggests that the catalytic decomposition of VOCs including this organic acid can be promoted to take place at mild conditions. Notice that formic acid may not be an important VOC but it represents a class of volatile organic molecules that can be easily quantified over this novel highly active catalyst for its catalytic destruction under the light activation.

As mentioned, a small amount of carbon monoxide in air is of great concern in confined space. However, catalytic CO oxidation at room temperature is challenging since CO and O₂ co-adsorption on metal surface are generally highly activated processes. It is interesting to note from the Fig. S5 that CO can be oxidised to CO₂ over Pd/PTH/C catalyst at room temperature by electromotive force. Fig. 8a also shows the significant promotion effect on the rate of CO oxidation to CO₂ in dilute O₂ over supported Pd on carbon with the addition of PTH with and without light illumination at much milder temperature range of 25-80°C. Thus, this represents an initial result demonstrating the enhancement of CO oxidation on the conductive polymer as a support. The reactor and conditions are yet to be optimised for such a conversion in order to produce a more practical device for the indoor pollution treatment.

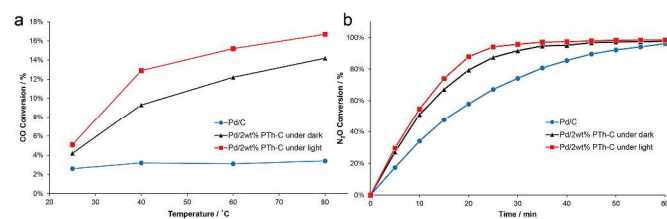


Fig. 8 (a) CO conversions over 50 mg of Pd/C and Pd/2 wt% PTH/C with and without illumination at different temperatures; 0.3 bar. with 2.60 % of CO and 5.0% O₂ in He; reaction time is 2 hours. (b) N₂O decomposition over 50 mg of Pd/C and Pd/2 wt% PTH/C with and without illumination at different times; 0.3 bar, with 2500 ppm N₂O, 4.75% Ar in 95% H₂ at RT.

The catalytic removal of trace N₂O is another challenging gas of environmental concern. A small amount of this gas can be produced from combustion engines or electrical discharge contaminating the quality of air. N₂O is known to dissociate on metal surface readily to N₂ and O_{ads} at room temperature but the strong O_{ads} could poison the metal surface instantly. It has been also reported that a small amount of H₂ co-fed to the metal catalyst can regenerate metal surface³³, which could be blended to the gas mixture or produced in-situ by electrochemical activation as similar described in Fig. 5a. As a result, a mixture of gas with 2500 ppm of N₂O in H₂ was used to probe the catalytic activity of the new composite material. As seen from Fig. 8b, Pd/C catalyst takes 57 minutes to achieve 95%

conversion while it takes 35 minutes for Pd/PTh-C catalyst to reach comparable conversion. Under light excitation < 25 minutes is required over the same but PTh promoted catalyst. Repeated testing of the composite comparing to the catalysis collected in dark condition was studied and is presented in Fig. S8. As seen from the figure that the ratio of N₂O decomposition activity with and without illumination reaches the highest at around 15 min at steady state but drops at further time due to the progressive consumption of N₂O in our batch reactor. In the period of no irradiation, there is no difference in the rate between two repeated dark experiments and the third period of irradiation, there is no sign of difference from the first period. Thus, there is no apparent deactivation for this cyclic testing. This may also suggest that there is no remained effect due to photolytic damage to the polythiophene during the irradiation and reaction.

Conclusions

In conclusion, in this preliminary work, we demonstrate the incorporation of polythiophene polymer as a support or support supplement can exert a significant electronic influence to metal nanoparticles embedded therein. The electronic modified supported Pd nanoparticles can render catalytic oxidation of CO, decomposition of N₂O and VOCs at much moderate conditions at higher rates due to the strong perturbation to the finite quantity of mobile electrons of the dispersed metal nanoparticles from the added polymer. In addition, the intrinsic visible light absorbing, highly thermal and electrical conductivity and mouldable nature of the conducting polymer can further facilitate selective catalysis at low temperature with different activation methods over a wide type of reactor systems. It is envisaged that this simple chemical modification can be applied directly to existing metal supported catalysts. It is also shown for the first time that the simple carbon supported Pd metal catalyst modified with the conductive polymer can give high activities for some important reactions of environmental concerns, outperforming those of conventional catalysts by the alternative means of activations. Apparently, there are further rooms for improvements for these preliminary findings in order to enhance the metal-polymer interactions for optimal catalysis (i.e. higher metal dispersion, dedicated functionalities for electronic interaction and more vigorous stability and mechanical strength, etc) With regards to the growing demands for greener catalysts for environmental pollutants and the limitations of versatile but active nanocatalysts at milder conditions, the surface modification of Pd by organic conductive polythiophene polymer via sulphur adsorption on the metal surface may thus find new uses in catalytic post-treatment of a wide range of hazardous chemicals.

Acknowledgements

The authors wish to thank the EPSRC, UK. WZ acknowledges China Scholarship Committee (CSC) for a visiting scholarship

to enable him to study at Oxford Univ. We also thank Dr. Ashley Shepherd (University of Oxford) for XPS testing, Dr. Simon Fairclough (University of Oxford) for EDX and TEM testing, and Mr. Yue Yu (Wuhan University) for SEM.

Notes and references

^a Wolfson Catalysis Centre, Department of Chemistry, University of Oxford, Oxford, OX1 3QR, UK.

^b College of Chemistry and Molecular Sciences, Wuhan University, Wuhan 430072, PRC.

*To whom correspondence should be addressed: Prof. Edman Tsang, E-mail: edman.tsang@chem.ox.ac.uk

Electronic Supplementary Information (ESI) available: [TEM images; EDX analysis of Pd-PTh composite; XPS characterization; Raman spectra; CO stripping voltammograms; ¹²C/¹³C adsorption ATR-FTIR test]. See DOI: 10.1039/b000000x/

1. H. Akimoto, *Science*, 2003, **302**, 1716–1719.
2. P. . Snytnikov, V. . Sobyenin, V. . Belyaev, P. . Tsyrlunikov, N. . Shitova, and D. . Shlyapin, *Appl. Catal. A Gen.*, 2003, **239**, 149–156.
3. L. Liu, F. Zhou, L. Wang, X. Qi, F. Shi, and Y. Deng, *J. Catal.*, 2010, **274**, 1–10.
4. S. Jones, J. Qu, K. Tedsree, X.-Q. Gong, and S. C. E. Tsang, *Angew. Chem. Int. Ed.*, 2012, **124**, 11437–11440.
5. T. A. Skotheim and J. Reynolds, *Conjugated Polymers: Theory, Synthesis, Properties, and Characterization*, CRC Press, 2006.
6. A. MacDiarmid, *Angew. Chem. Int. Ed.*, 2001, **40**, 2581–2590.
7. J. Peet, J. Y. Kim, N. E. Coates, W. L. Ma, D. Moses, a J. Heeger, and G. C. Bazan, *Nat. Mater.*, 2007, **6**, 497–500.
8. J. Roncali, *Chem. Rev.*, 1997, **97**, 173–206.
9. T. Maruyama and T. Yamamoto, *J. Phys. Chem. B*, 1997, **5647**, 3806–3810.
10. X. Wang, K. Maeda, A. Thomas, K. Takanabe, G. Xin, J. M. Carlsson, K. Domen, and M. Antonietti, *Nat. Mater.*, 2009, **8**, 76–80.
11. T. Kawai, T. Kuwabara, and K. Yoshino, *J. Chem. Soc., Faraday Trans.*, 1992, **88**, 2041–2046.
12. B. Muktha, G. Madras, T. N. G. Row, U. Scherf, and S. Patil, *J. Phys. Chem. B*, 2007, **111**, 7994–7998.
13. J.-X. Jiang, C. Wang, A. Laybourn, T. Hasell, R. Clowes, Y. Z. Khimyak, J. Xiao, S. J. Higgins, D. J. Adams, and A. I. Cooper, *Angew. Chem. Int. Ed.*, 2011, **50**, 1072–1075.
14. C. Moorlag, B. C. Sih, T. L. Stott, and M. O. Wolf, *J. Mater. Chem.*, 2005, **15**, 2433–2436.
15. L. Zhai and R. D. McCullough, *J. Mater. Chem.*, 2004, **14**, 141–143.
16. T. Xu and Q. Qiao, *Energy Environ. Sci.*, 2011, **4**, 2700–2720.
17. K. R. Edelman, K. J. Stevenson, and B. J. Holliday, *Macromol. Rapid Commun.*, 2012, **33**, 610–615.
18. S. Harish, J. Mathiyarasu, K. L. N. Phani, and V. Yegnaraman, *Catal. Letters*, 2008, **128**, 197–202.
19. S. Fujii, M. Kodama, and S. Matsuzawa, in *Advances in Nanocomposite Technology*, ed. A. Hashim, 2011.

Journal Name

20. C. K. Yong, K. Noori, Q. Gao, H. J. Joyce, H. H. Tan, C. Jagadish, F. Giustino, M. B. Johnston, and L. M. Herz, *Nano Lett.*, 2012, **12**, 6293–301.
21. J. C. Scott, *J. Vac. Sci. Technol. A Vacuum, Surfaces, Film.*, 2003, **21**, 521–531.
22. M. T. Giacomini, E. a. Ticianelli, J. McBreen, and M. Balasubramanian, *J. Electrochem. Soc.*, 2001, **148**, A323–A329.
23. M. T. Giacomini, M. Balasubramanian, S. Khalid, J. McBreen, and E. A. Ticianellia, *J. Electrochem. Soc.*, 2003, **150**, A588–A593.
24. S. Jung, H. Jung, J. Ho, H. Kim, S. Sung, B. Yoo, D. Ha, C. Lee, and Y. Lee, *J. Electroanal. Chem.*, 2011, **655**, 39–44.
25. Y. Gao, C.-A. Chen, H.-M. Gau, J. A. Bailey, E. Akhadov, D. Williams, and H.-L. Wang, *Chem. Mater.*, 2008, **20**, 2839–2844.
26. K. Mallick, K. Mondal, M. Witcomb, and M. Scurrall, *J. Mater. Sci.*, 2008, **43**, 6289–6295.
27. X.-G. Li, J. Li, Q.-K. Meng, and M.-R. Huang, *J. Phys. Chem. B*, 2009, **113**, 9718–9727.
28. D. Kelkar and A. Chourasia, *Chem. Chem. Technol.*, 2011, **5**, 309–315.
29. I. F. Perepichka, D. F. Perepichka, H. Meng, and F. Wudl, *Adv. Mater.*, 2005, **17**, 2281–2305.
30. A. Ortega, F. M. Hoffman, and A. M. Bradshaw, *Surf. Sci.*, 1982, **119**, 79–94.
31. H. Ishii, K. Sugiyama, E. Ito, and K. Seki, *Adv. Mater.*, 1999, **11**, 605–625.
32. K. Tedsree, T. Li, S. Jones, C. W. A. Chan, K. M. K. Yu, P. a J. Bagot, E. a Marquis, G. D. W. Smith, and S. C. E. Tsang, *Nat. Nanotechnol.*, 2011, **6**, 302–307.
33. R. Burch, G. a Attard, S. T. Daniells, D. J. Jenkins, J. P. Breen, and P. Hu, *Chem. Commun.*, 2002, **44**, 2738–2739.